CHEMISTRY
A EUROPEAN JOURNAL

DOI: 10.1002/chem.200903239

# Direct Observation of Molecular-Level Template Action Leading to Self-Assembly of a Porous Framework

Sneha R. Bajpe,*[a] Christine E. A. Kirschhock,*[a] Alexander Aerts,[a] Eric Breynaert,[a] Gregory Absillis,[b] Tatjana N. Parac-Vogt,[b] Lars Giebeler,[a] and Johan A. Martens[a]

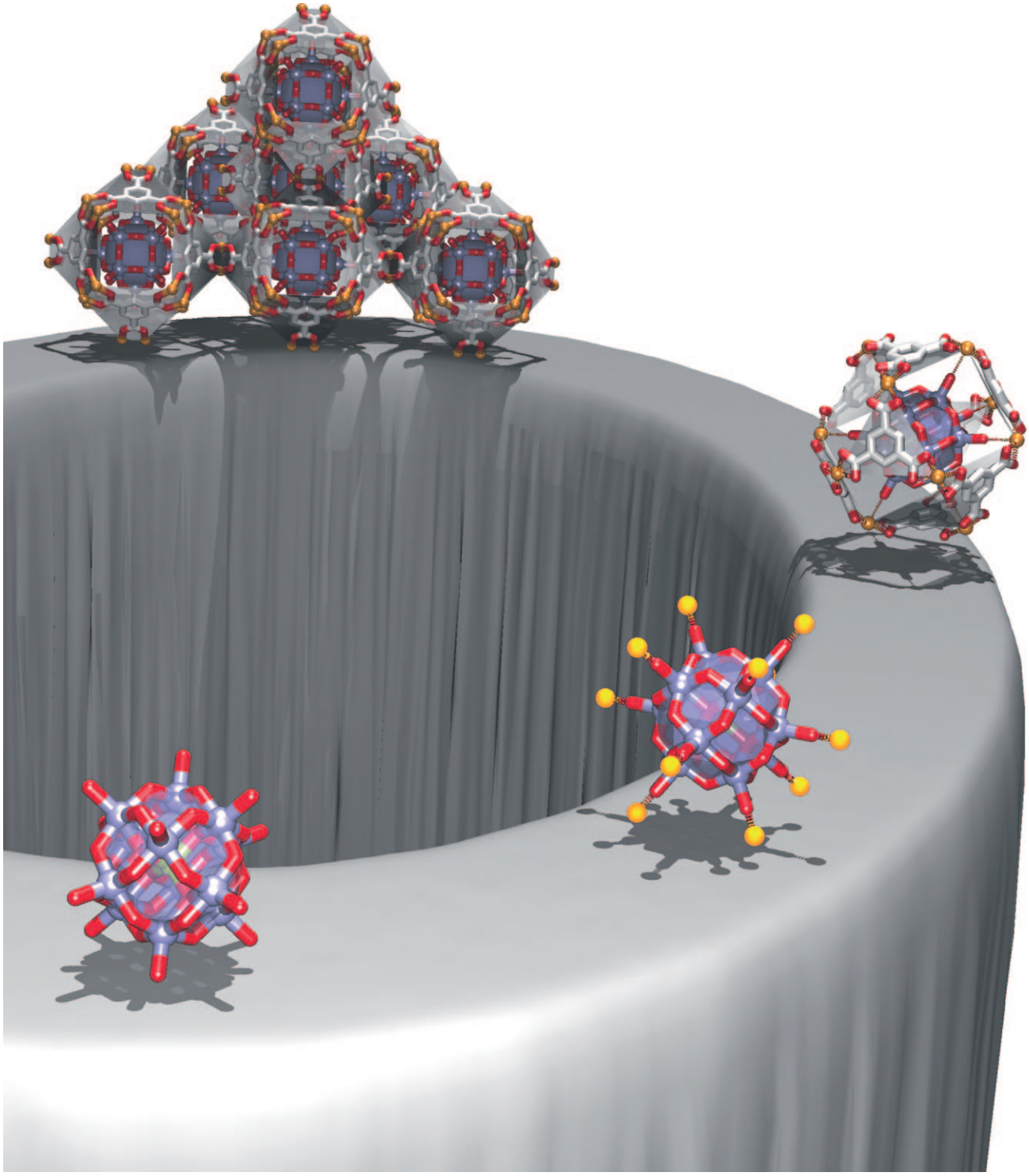

**Abstract:** The molecular steps involved in the self-assembly of $Cu_3(BTC)_2$ (BTC = 1,3,5-benzenetricarboxylic acid) metal–organic frameworks that enclose Keggin-type $H_3PW_{12}O_{40}$ heteropolyacid molecules were unraveled by using solution $^{17}O$, $^{31}P$, and $^{183}W$ NMR spectroscopy, small-angle X-ray scattering, near-IR spectroscopy, and dynamic light scattering. In aqueous solution, complexation of $Cu^{2+}$ ions with Keggin-type heteropolyacids was observed. $Cu^{2+}$ ions are arranged around the Keggin structure so that linking through benzenetricarboxylate groups results in the formation of the $Cu_3(BTC)_2$ MOF structure HKUST-1. This is a unique instance in which a templating mechanism that relies on specific molecular-level matching and leads to explicit nanoscale building units can be observed in situ during formation of the synthetic nanoporous material.

**Keywords:** keggin heteropolyacids · NMR spectroscopy · polyoxometalates · metal–organic frameworks · template synthesis

## Introduction

In the everyday world, a template is considered to be a mould in which a malleable substance can be patterned into a specific shape. Structure templating is a common theme in biochemistry. For example, all DNA polymerase reactions depend on an appropriate DNA template for self-replication.[1,2] In the inanimate world, the use of templates is also a common synthesis strategy. Mastering control over pore topology during framework formation is of crucial importance, particularly for the design of nanoporous heterogeneous catalysts and adsorbents[3–6] In this context, a real template can be defined as an agent that favors formation of a specific open framework under a broad range of conditions and that accelerates crystallization.[7] Deeper understanding of the template mechanisms of porous structures is a highly coveted goal to rationalize the synthesis of materials like zeolites[3–6] or metal–organic frameworks (MOFs).[8–17] Molecules ending up in the pores of a microporous material upon synthesis could act as unspecific void fillers,[4,18–19] or modify solvent properties,[19] or directly arrange framework components into specific building units that lead to the final framework. Although the first two actions have been observed experimentally, a direct structure direction based on molecular-level self-organization, reminiscent of biological systems, remains elusive. In such an instance the template should already carry information about the topology of the final framework that is then imprinted on the forming structure.[20] Herein we present the observation of such a direct template mechanism that enforces the assembly of a specific MOF.

MOFs are porous materials composed of metal ions or clusters linked by organic ligands.[21] Porosity is imposed by the rigidity of the linkers and the specific coordination geometry around the metal ions, rather than by the presence of structure-directing agents. However, some authors have also reported the successful use of templates in MOF synthesis. In most of these cases, the solvent behaves as a void-filling agent.[18] A variation in the solvent properties, such as addition of dimethylformamide,[19] can also have a beneficial influence on the formation of MOFs and, in some cases, a variation in solubility can even enable synthesis at room temperature.[19] However, a specific molecular-level manipulation of framework components by a synthesis additive has not been observed yet. Herein we report the detailed mechanism of direct molecular-level templating that leads to specific building units and eventually to the construction of a MOF material. The structure-directing action turns the hydrothermal synthesis of $Cu_3(BTC)_2$ (BTC = 1,3,5-benzenetricarboxylic acid)[22] into a room-temperature self-assembly process.

## Results and Discussion

Sun et al. reported that Keggin-type heteropolyacids (HPAs) can be incorporated in $Cu_3(BTC)_2$ during hydrothermal synthesis.[23] Examples of occluded HPAs are $H_{8-x}XM_{12}O_{40}$ ($X = Si^{4+}$ or $P^{5+}$, $x = 4$ (Si) or 5 (P), $M = Mo^{6+}$ or $W^{6+}$). Unlike examples in which the HPA ions partially disintegrate before assembly into supramolecular structures,[14,24] the Keggin ions remain fully intact in the $Cu_3(BTC)_2$ cages. During closer inspection of the structures, we recognized a striking relationship between the geometries of the Keggin-type HPA and the two cavities of the $Cu_3(BTC)_2$ framework. The terminal oxygen atoms ($O_{term}$) of the HPA anion point directly towards 12 Cu pairs that are the nodes of one of the two cuboctahedral $Cu_3(BTC)_2$ cavities (Figure 1).

Intrigued by those structures and inspired by the concept of supramolecular chemistry,[14,25] we prepared an aqueous

[a] S. R. Bajpe, Prof. C. E. A. Kirschhock, Dr. A. Aerts, Dr. E. Breynaert, Dr. L. Giebeler, Prof. J. A. Martens
Centre for Surface Science and Catalysis
Department of Microbial and Molecular Systems
K. U. Leuven, Kasteelpark Arenberg 23
Leuven B-3001 (Belgium)
Fax: (+32) 16-321062
E-mail: Christine.Kirschhock@biw.kuleuven.be
Sneha.BajpeRohita@biw.kuleuven.be

[b] G. Absillis, Prof. T. N. Parac-Vogt
Molecular Design and Synthesis
Department of Chemistry
K. U. Leuven, Celestijnenlaan 200 F
Leuven B-3001 (Belgium)

Supporting information for this article is available on the WWW under http://dx.doi.org/10.1002/chem.200903239.

  

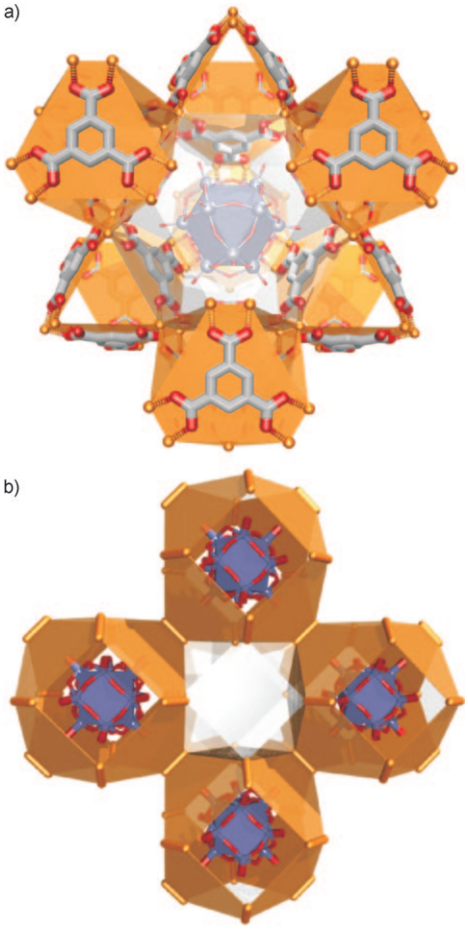


Figure 1. Keggin-type HPA molecule enclosed in $Cu_3(BTC)_2$. The HPA is represented in blue, Cu atoms in gold, oxygen atoms in red, and carbon in white. Cu pairs linked by BTC are symbolized by gold triangles. a) One cavity containing HPA viewed along [111], b) arrangement of the two types of cavities viewed along [100].

solution of $Cu(NO_3)_2{\cdot}3H_2O$ to which we successively added an aqueous solution of HPA ($H_3PW_{12}O_{40}$, $H_4SiW_{12}O_{40}$, or $H_3PMo_{12}O_{40}$) and BTC. At room temperature, the instantaneous and stoichiometric formation of a $Cu_3(BTC)_2$-type metal–organic framework with intact HPA molecules positioned in the MOF pores occurred. The product showed superior crystallinity compared with samples synthesized hydrothermally.[23] No 3D framework formed in the absence of HPA, in agreement with earlier observations.[26] The synthesis also failed if BTC was added prior to HPA. The importance of the preparation sequence was an indication that HPA takes the role of prearranging the $Cu^{2+}$ ions. It was speculated that a $Cu^{2+}$/HPA interaction directs the $Cu^{2+}$ ions to preferentially reside close to positions needed to build the MOF framework. In such a scenario, the role of the organic linker is simply to connect the already structured $Cu^{2+}$/HPA units by complexation. In fact, after the addition of BTC to the $Cu^{2+}$/HPA solution and within the short time necessary to place the sample into the laser (1–2 min) of a dynamic light scattering (DLS) instrument, 300–500 nm sized particles had already formed. Powder X-ray diffraction (PXRD) of the suspension showed these particles to be crystalline $Cu_3(BTC)_2$ (Figure S1 in the Supporting Information). Immediately after formation, the crystals show cubic habits (Figure 2a), but after stirring the suspension for one day the crystals assumed octahedral shape with outstanding crystallinity (Figure 2b) as derived from the small linewidth of the Bragg reflections (Figure S2 in the Supporting Information).

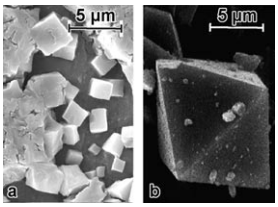


Figure 2. SEM images showing particle formation a) within 1–2 min after BTC addition to the $Cu^{2+}$/HPA solution and b) after stirring the reaction mixture for 1 d.

Direct evidence of strong interaction between $Cu^{2+}$ and HPA ions was obtained from $^{31}P$ NMR spectra of solutions prepared from $Cu(NO_3)_2{\cdot}3H_2O$ and $H_3PMo_{12}O_{40}{\cdot}xH_2O$. In the presence of $Cu^{2+}$ cations, the $^{31}P$ resonance of the Keggin polyanion showed a significant shift of 0.72 ppm (Figure 3b). Such a prominent impact on the local environment of the central P atom in the HPA can only be the result of a strong electrostatic interaction with $Cu^{2+}$ cations. Upon adding BTC to this solution, a slightly smaller shift in

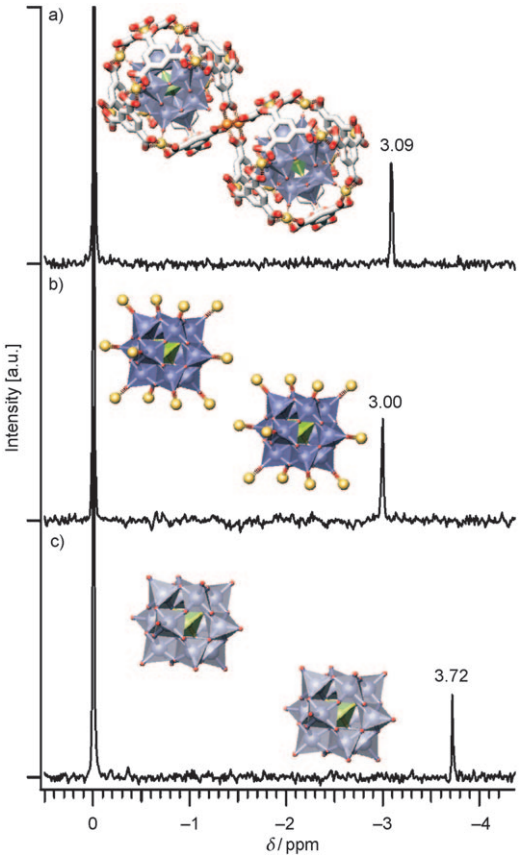


Figure 3. $^{31}P$ NMR spectra of c) a solution of $H_3PMo_{12}O_{40}{\cdot}xH_2O$, b) a solution of $Cu(NO_3)_2{\cdot}3H_2O$ and $H_3PMo_{12}O_{40}{\cdot}xH_2O$, and a) solution b) after BTC addition. The signal at $\delta = 0$ ppm is due to the external reference (85% phosphoric acid).

  

the $^{31}P$ NMR signal indicated a somewhat reduced $Cu^{2+}$/HPA polyanion interaction (Figure 3a), presumably due to the coordination of the BTC linker to $Cu^{2+}$. Substantial evidence was further obtained from the $^{183}W$ NMR spectra, which showed a significant shift pertaining to the strong electrostatic interaction between the $Cu^{2+}$ and tungsten in the HPA (Figure 4). Only one $^{183}W$ signal was measured,

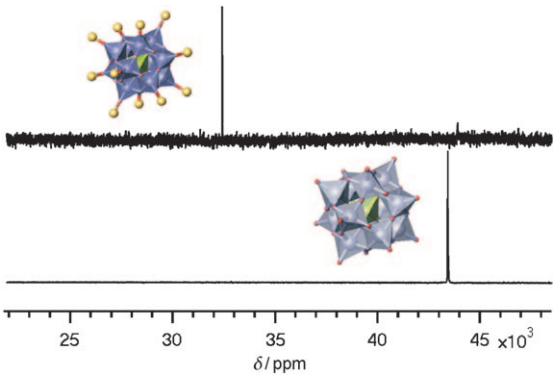


Figure 4. $^{183}W$ NMR spectra of a solution of $Cu(NO_3)_2 \cdot 3H_2O$ with $H_3PW_{12}O_{40} \cdot x H_2O$ (top) that shows a shift with respect to the $H_3PW_{12}O_{40} \cdot x H_2O$ solution (bottom).

which confirms the presence of only one type of W environment and indicates that the Keggin ions are fully intact. After addition of the linker molecule, unequivocal confirmation of BTC binding to $Cu^{2+}$ was obtained from the $^1H$ NMR spectra. A large broadening and downfield shift of the BTC proton resonance from $\delta = 8.80$ to 9.26 ppm upon addition to $Cu^{2+}$/HPA solution pointed to the coordination of BTC by $Cu^{2+}$ ions (Figure S3 in the Supporting Information).

Additional details about the type of $Cu^{2+}$/HPA interaction before BTC addition were derived from $^{17}O$ NMR of a solution with substoichiometric concentration of $Cu^{2+}$ with respect to HPA ($Cu^{2+}$/HPA molar ratio of 80%). This allowed observation of resonances of free HPA next to interacting species in the same spectrum (Figure 5). A solution of pure $Cu(NO_3)_2 \cdot 3H_2O$ gave no $^{17}O$ NMR signal due to fast exchange of the water molecules in the vicinity of the paramagnetic $Cu^{2+}$ ion that caused rapid relaxation, extensive signal broadening, and quenching. However, in the presence of HPA a well-resolved spectrum with a strong water signal was observed (Figure 5). This is a clear hint that the majority, if not all, of the $Cu^{2+}$ ions no longer partake in fast exchange of water.

The $^{17}O$ NMR spectrum of a free $PW_{12}O_{40}^{3-}$ anion should, due to its symmetrical structure, consist of only four $^{17}O$ signals corresponding to terminal oxygens ($O_{term}$), corner- and edge-sharing bridging oxygens ($O_{bridge}$), and core oxygens linked to the tetrahedrally coordinated central atom. The $^{17}O$ NMR spectrum of the $PW_{12}O_{40}^{3-}$ anion at pH 1.6 showed two very broad signals at $\delta = 722$ and 398 ppm, which indicate a fast intramolecular exchange involving both $O_{term}$ ($\delta = 722$ ppm) and $O_{bridge}$ ($\delta = 398$ ppm) atoms[27] under these acidic conditions (Figure S4 in the Supporting Information).

Addition of $Cu^{2+}$ to $PW_{12}O_{40}^{3-}$ had a profound effect on the $^{17}O$ NMR spectrum, resulting in the appearance of several sharp $^{17}O$ resonances (Figure 5). The significant sharpening of the $^{17}O$ NMR signals upon addition of $Cu^{2+}$ clearly suggested that an intramolecular oxygen exchange within the HPA was hindered due to the presence of $Cu^{2+}$. No other resonances occurred in the region of the chemical shift of $O_{term}$, which allowed a more detailed analysis. Four signals were clearly observed: the free HPA at $\delta = 717$ ppm and three shifted signals with an intensity ratio ($I_{shifted}/I_{total}$) of 82%, mirroring the initial $Cu^{2+}$/HPA ratio of 4:5. This confirmed quantitative binding of all available $Cu^{2+}$ ions to one HPA anion each. The splitting of the shifted signals was caused by the strong interaction with $Cu^{2+}$ breaking the symmetry of the structure. The break in symmetry can only be observed if equivalent oxygen atoms have different environments on the timescale of the NMR experiment, which proved that the $Cu^{2+}$ ions resided for a long time at the same positions relative to the Keggin ion. Analysis of the intensities of the shifted signals revealed this location; a ratio of roughly 4:2:5 was observed at chemical shifts of $\delta = 655$, 700, and 706 ppm, respectively. A shoulder on the signal at

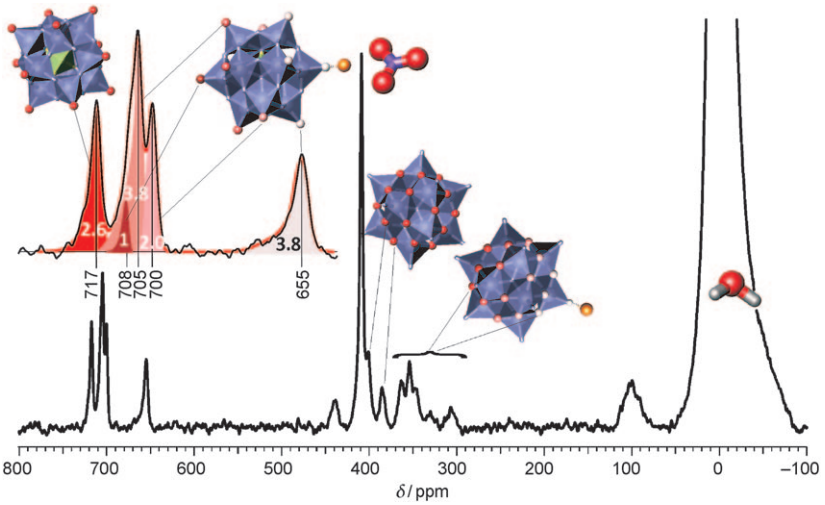


Figure 5. $^{17}O$ NMR spectrum of $Cu(NO_3)_2$/HPA (molar ratio of $Cu^{2+}$/HPA: 80%). The shading of the oxygen atoms of the Keggin ions interacting with $Cu^{2+}$ symbolizes the strength of impact of the $Cu^{2+}$ ion. The strong, sharp signal around $\delta = 420$ ppm was identified as a nitrate. The HPA is represented in blue, Cu atoms in gold, oxygen atoms in shades of red, nitrogen in blue, and hydrogen in light grey.

$\delta = 706$ ppm hinted at two types of oxygen atoms present in a ratio of 4:1, with one being least affected by the presence of $Cu^{2+}$. Comparison with the geometry of the Keggin ion left only one conclusion, that $Cu^{2+}$ binds to $O_{term}$, with the resonance of the bound oxygen ($O_{term}$*) being quenched due to paramagnetic interaction. Though the signals in the region of bridging oxygens were not analyzed in detail, the shifted signals were in accordance with the deduced location of $Cu^{2+}$. The resonances of the four $O_{bridge}$ atoms on the same octahedron as the $O_{term}$* atoms were significantly broadened due to their close proximity to the paramagnetic transition-metal ion ($\delta = 300$–$340$ ppm).

To perceive the $Cu^{2+}$/HPA interaction from the viewpoint of copper, near-infra red (NIR) spectroscopy measurements were performed. A blueshift as a function of varying the ratio of HPA to $Cu^{2+}$ indicated a change in the coordination geometry of $Cu^{2+}$(Figure 6). For comparison, an acidified solution of $Cu^{2+}$ did not show a shift, which confirms that the change in coordination of the $Cu^{2+}$ species was indeed caused by strong interaction with HPA anions.

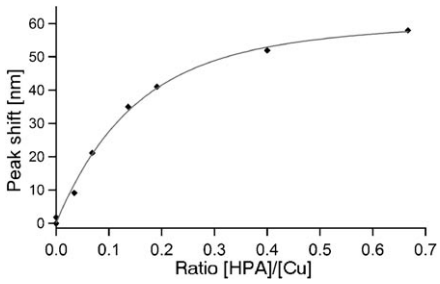


Figure 6. NIR measurements of an $Cu^{2+}$/HPA solution with varying amounts of HPA. The blueshift indicates the formation of lower coordination number species.

If indeed the $Cu^{2+}$ ions firmly associate with the Keggin polyanions, the assembly should show increased size and different diffusivity compared to free Keggin ions. To confirm this, small-angle X-ray scattering (SAXS) and DLS experiments were performed on HPA and $Cu^{2+}$/HPA solutions. A simple model accounting for monodisperse spheres and electrostatic interaction could perfectly describe the SAXS data (Figure 7). The diameter of pure Keggin polyanions has been determined to be 1.06 nm (Figure 7b) which exactly agrees with the crystallographic structure.[28] A maximum in the scattering curve clearly indicates electrostatic interaction between charged polyanions. When $Cu^{2+}$ was added, the particle diameter increased to 1.22 nm (Figure 7a) and the electrostatic interactions were shielded. In accordance with these results, diffusion constants derived from the DLS correlation functions indicated strongly reduced polyanion diffusivity after addition of $Cu^{2+}$ (Figure S5 in the Supporting Information).

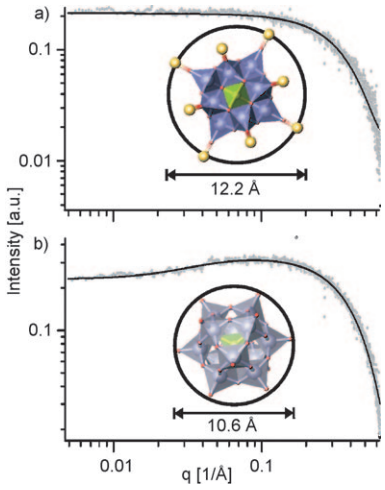


Figure 7. SAXS results showing a simple model fit for the monodisperse sphere and electrostatic interaction, which accounts for the increase in particle diameter of $Cu^{2+}$/HPA solution. The HPA is represented in blue, Cu atoms in gold, and oxygen atoms in red.

Consistent results from NMR, SAXS, DLS, and NIR experiments left us to conclude that HPA ions act as structure-directing agent by defining the position of $Cu^{2+}$ ions before the BTC ligand is added. The organic linkers then consolidate the Cu positions by coordination and, in a last step, the building units assemble rapidly into a final crystalline material (Figure 8). Until now, the same scenario has been encountered for three different types of HPAs: $H_3PMo_{12}O_{40}$, $H_3PW_{12}O_{40}$, and $H_4SiW_{12}O_{40}$ (Figure S6 in the Supporting Information). Silicotungstic polyanions carry a charge of 4− compared with 3− for the phosphorus-based Keggin species. The difference in charge appears to have no effect on the structure-directing power during MOF formation. All structures were confirmed by Rietveld refinement of PXRD data based on data known from hydrothermal synthesis (Figure S7 in the Supporting Information).[23] As can be seen in Figures 1b and 8, the $Cu_3(BTC)_2$ framework consists of two types of large cavity that differ in the orientation of the linker molecules and Cu pairs. According to Rietveld refine-

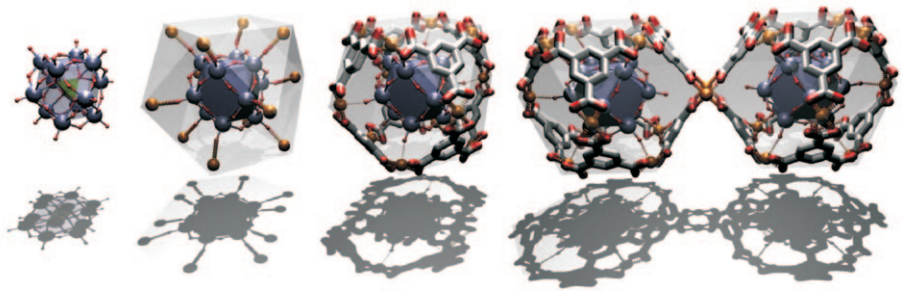

Figure 8. Structure-directing behavior of HPA on $Cu^{2+}$ during formation of a MOF (an animated visualization is available as part of the Supporting Information).

ment (Figure S7 in the Supporting Information) and the literature,[23] Keggin ions only reside in those cavities in which the BTC molecules are in plane with the cavity wall. This is a direct consequence of the presented model in which copper is first pre-arranged, then linked during the formation of a cavity and finally reorganized into paddlewheels composed of two $Cu^{2+}$ ions and four BTC molecules during structure assembly (Figure 8). In the final three-dimensional network, water is found in the other type of large cavity within interaction distance with the $Cu^{2+}$ ions that point directly into these cages. The porosity of $Cu_3(BTC)_2$ and HPA-incorporated $Cu_3(BTC)_2$ samples were established by nitrogen sorption data (Figure S8 in the Supporting Information). Elemental analysis of the samples fully confirmed these results. For example, the ratio of Cu/P/Mo determined by ICP analysis was 48:5.9:48.6, which is in good agreement with the theoretical ratio of 48:4:48 for Cu/P/Mo.

## Conclusion

We have presented evidence for molecular-level structure templating by using the example of self-assembly of a MOF material that encapsulates Keggin-type HPAs. Even though the use of void-filling templates for synthesis of MOFs has been conceived[18,29–30] and some structures have been prepared at room temperature by changing the solvent properties,[19,31] insight in the molecular-level mechanism that results in templating of a 3D porous framework has, to our knowledge, not yet been provided in such detail. The actual role of templates in zeolite synthesis has been investigated for decades,[32,33] but active structure direction on the molecular level also remained hypothetical. With Keggin-type HPAs, the molecular mechanism for the spatial organization[34] of the transition metal by the template is obvious. Besides the high importance of the confirmation of specific, molecular-level templating as a viable pathway towards porous materials, we also discovered the surprisingly strong physicochemical interaction between Keggin and $Cu^{2+}$ ions.

This observation could open a new supramolecular approach to HPAs with other transition metals and organic linkers and could result in a wide diversity of materials with already inbuilt HPA and polyoxometalate chemistry in general. Our study has shown that it is possible to analyze the dynamics of molecular interaction of HPAs and transition-metal ions with high precision. Herein, this allowed the conditions to be tuned for successful synthesis of a variety of HPAs incorporated in one type of MOF. This success implies the possible extension of this strategy for applications in acid and redox catalysis as well as gas absorption. It is highly probable that the simplicity of the preparation procedure will open a whole range of new opportunities, such as patterned deposition, deposition on cloths and textiles, or casting of films, just by simple impregnation with the transition metal–HPA precursor before linker addition and precipitation.

## Experimental Section

**Materials**: BTC was purchased from Acros Organics. The solvents were purchased from VWR Scientific Products, Leuven (Belgium). All other materials were obtained from Fluka and used without further purification.

**Synthesis of HPA-incorporated MOFs at RT**: An aqueous solution of $Cu(NO_3)_2{\cdot}3H_2O$ (0.13 M, 10 mL) was prepared, then a solution of HPA (0.01 M, 6.4 mL) in water was added and the mixture was stirred for 5 min. The pH of the solution was maintained at $\approx$1.6 by adding aqueous NaOH. BTC (0.1 M) in ethanol (13.3 mL) was added and stirred for 24 h at RT. The precipitate was filtered, repeatedly washed with water, and dried at 40 °C. The reactant weights, reagent volume, solution pH, stirring period, and the sequence of addition of each solution were optimized. Stirring for a longer period of time (1 to 6 d) did not show any changes in the reaction products.

**Synthesis of HPA incorporated MOFs by hydrothermal route**: Aqueous $Cu(NO_3)_2{\cdot}3H_2O$ (0.13 M, 10 mL) was mixed with a solution of HPA (0.01 M, 6.4 mL) in water was added and stirred for 5 min. While the pH was maintained at $\approx$1.6, BTC (0.1 M) in pure ethanol (13.3 mL) was added. The mixture was stirred for 30 min at RT, then placed in teflon-lined stainless steel autoclaves and heated to 110 °C for 15 h at a rate of 1 °C $min^{-1}$, then finally allowed to cool for a day. The reaction product was then filtered and repeatedly washed with water before drying at 40 °C.[35]

**$^{31}$P, $^{17}$O and $^{183}$W NMR spectroscopy**: $^{31}$P NMR spectra were recorded at 162 MHz by using a Bruker Avance 400 spectrometer. Phosphoric acid (85 %) was used as an external reference. The amounts of $Cu(NO_3)_2{\cdot}3H_2O$, HPA, and BTC used were the same as those used in the synthesis. The solutions were prepared in $D_2O$ and the pH of the solution mixture was maintained at 1.6. $^{17}$O NMR spectra were recorded at 81 MHz by using a Bruker Avance 600 spectrometer. A solution of HPA (0.5 M) and $Cu(NO_3)_2{\cdot}3H_2O$ (0.4 M) was prepared in $D_2O$ (3 mL) at a pH of 1.6, and the solvent $^{17}$O NMR signal was used as the $\delta = 0$ ppm reference. $^{183}$W NMR spectra were recorded at 25 MHz by using a Bruker Avance 600 spectrometer. The concentration of the solutions of $Cu^{2+}$ and the HPA in $D_2O$ were the same as in the preparation procedure. $Na_2WO_4$ (2 M) in $D_2O$ was used as an external reference.

**SAXS**: SAXS patterns of samples placed in a 1 mm vacuum-tight quartz capillary were measured at RT by using a SAXSess mc$^2$ instrument (Anton Paar, Graz, Austria) with line-collimated $Cu_{K\alpha}$ radiation and a CCD detector. SAXS patterns were normalized to incident beam intensity. Concentrations and ratios of $Cu(NO_3)_2{\cdot}3H_2O$ and HPA were the same as during synthesis and $^{31}$P NMR spectroscopy. The scattering of water and aqueous $Cu(NO_3)_2{\cdot}3H_2O$ (0.13 M) was subtracted as background for the HPA ($H_3PW_{12}O_{40}{\cdot}x\,H_2O$) and $Cu^{2+}$/HPA samples, respectively. Background subtraction and correction for instrumental broadening was performed by using the SAXSquant software. Model fits were performed by using the NIST SANS package for the Igor Pro software (Wavemetrics).[36] The form factor of monodisperse spheres and the Hayter–Penfold structure factor for electrostatic interactions were used.

**DLS**: An ALV/CGS-3 instrument (ALV, Langen, Germany) was used for DLS measurements. A solution of $H_3PW_{12}O_{40}{\cdot}x\,H_2O$ (0.01 M) and $Cu(NO_3)_2{\cdot}3H_2O$ (0.13 M) was prepared in filtered Millipore water (16.4 mL) by using 20 nm Whatman Teflon antop syringe filters. The samples were then filtered by using 100 nm Whatman Teflon syringe filters and measured in glass tubes that had previously been cleaned with filtered acetone (100 nm Whatman filters) and dried to avoid any interference of dust particles in the samples. After inserting the sample in the instrument, 5 min were allowed for temperature stabilization. Light with a wavelength of 659 nm was used. Measurements of 60 s were performed at three different angles of 30, 90, and 150°. Because the HPA gave very weak signals due to very small particles, measurements were repeated over 24 h for both the HPA and $Cu^{2+}$/HPA solutions.

**NIR spectroscopy**: A UV/Vis Lambda 12 Perkin–Elmer instrument was used to measure samples with varying amounts of $H_3PW_{12}O_{40}{\cdot}x\,H_2O$/$Cu(NO_3)_2{\cdot}3H_2O$ with the concentration of $Cu(NO_3)_2{\cdot}3H_2O$ (0.03 M) kept

  

constant. The solutions were prepared in Millipore water and the measurements were conducted within a range of $\lambda = 600$–$900$ nm.

## Acknowledgements

J.A.M. acknowledges the Flemish Government for long-term structural funding (Methusalem). The work was supported by Excellence funding (CECAT), a concerted research action (GOA), and an FWO project. A.A. and E.B. acknowledge the Flemish FWO for a postdoctoral fellowship. G.A. acknowledges the Flemish FWO for a doctoral fellowship. We thank Jan Vermant for providing us with facilities to use the ALV/LSE-5003 light scattering instrument. We also thank Heiner Santner and Heimo Schnablegger of Anton Paar (Austria) for the SAXS measurements with the SAXSess instrument and Wim De Borggraeve and Karel Duerinckx for help with NMR measurements.

[1] J. M Berg, J. L. Tymoczko, L. Stryer, N. D. Clarke, *Biochemistry*, Freeman, Boston, **2002**, Chapter 27.
[2] B. Alberts, A. Johnson, J. Lewis, M. Raff, K. Roberts, P. Walter, *Molecular Biology of the Cell*, Garland Science, New York, **2002**, Chapter 5.
[3] X. S. Zhao, F. Su, Q. Yan, W. Guo, X. Y. Bao, L. Lv, Z. Zhou, *J. Mater. Chem.* **2006**, *16*, 637–648.
[4] G. Férey, *Chem. Soc. Rev.* **2008**, *37*, 191–214.
[5] J. Pérez-Ramírez, C. H. Christensen, K. Egeblad, C. H. Christensen, J. C. Groen, *Chem. Soc. Rev.* **2008**, *37*, 2530–2542.
[6] G. J. de A. A. Soler-Illia, C. Sanchez, B. Lebeau, J. Patarin, *Chem. Rev.* **2002**, *102*, 4093–4138.
[7] P. Jacobs, J. Martens, *Stud. Surf. Sci. Catal.* **1987**, *33*, 61.
[8] M. J. Rosseinsky, *Microporous Mesoporous Mater.* **2004**, *73*, 15–30.
[9] J. J. Perry IV, J. A. Perman, M. J. Zaworotko, *Chem. Soc. Rev.* **2009**, *38*, 1400–1417.
[10] J. Y. Lee, O. K. Farha, J. Roberts, K. A. Scheidt, S. T. Nguyen, J. T. Hupp, *Chem. Soc. Rev.* **2009**, *38*, 1450–1459.
[11] D. V. Soldatov, *J. Chem. Crystallogr.* **2006**, *36*, 747–768.
[12] G. K. H. Shimizu, *J. Solid State Chem.* **2005**, *178*, 2519–2526.
[13] J. R. Long, O. M. Yaghi, *Chem. Soc. Rev.* **2009**, *38*, 1213–1214.
[14] S. L. James, *Chem. Soc. Rev.* **2003**, *32*, 276–288.
[15] A. Müller, H. Reuter, S. Dillinger, *Angew. Chem.* **1995**, *107*, 2505–2539; *Angew. Chem. Int. Ed. Engl.* **1995**, *34*, 2328–2361.
[16] S. Kitagawa, R. Kitaura, S. Noro, *Angew. Chem.* **2004**, *116*, 2388–2430; *Angew. Chem. Int. Ed.* **2004**, *43*, 2334–2375.
[17] S. Kaskel, *Handbook of Porous Solids, Vol. 2* (Eds: F. Schüth, K. S. W. Sing, J. Weitkamp), Wiley-VCH, Weinheim. **2002**, p. 1190.
[18] D. T. de Lill, N. S. Gunning, C. L. Cahill, *Inorg. Chem.* **2005**, *44*, 258–266.
[19] D. J. Tranchemontagne, J. R. Hunt, O. M. Yaghi, *Tetrahedron* **2008**, *64*, 8553–8557.
[20] J.-M. Lehn, *Chem. Soc. Rev.* **2007**, *36*, 151–160.
[21] O. M. Yaghi, G. Li, H. Li, *Nature* **1995**, *378*, 703–706.
[22] S. S.-Y. Chui, S. M.-F. Lo, J. P. H. Charmant, A. G. Orpen, I. D. Williams, *Science* **1999**, *283*, 1148–1150.
[23] C.-Y. Sun, S.-X. Liu, D.-D. Liang, K.-Z. Shao, Y.-H. Ren, Z.-M. Su, *J. Am. Chem. Soc.* **2009**, *131*, 1883–1888.
[24] A. Müller, S. K. Das, H. Bögge, M. Schmidtmann, A. Botar, A. Patrut, *Chem. Commun.* **2001**, 657–658.
[25] J.-M. Lehn, *Supramolecular Chemistry: Concepts and Perspectives*, VCH, Weinheim. **1995**.
[26] E. Biemmi, C. Scherb, T. Bein, *J. Am. Chem. Soc.* **2007**, *129*, 8054–8055.
[27] I. V. Kozhevnikov, *Chem. Rev.* **1998**, *98*, 171–198.
[28] J. F. Keggin, *Proc. R. Soc. London Ser. A* **1934**, *144*, 75–100.
[29] C. Serre, C. Mellot-Draznieks, S. Surblé, N. Audebrand, Y. Filinchuk, G. Férey, *Science* **2007**, *315*, 1828–1831.
[30] M. Franck, C. Serre, N. Guillou, G. Férey, R. I. Walton, *Angew. Chem.* **2008**, *120*, 4168–4173; *Angew. Chem. Int. Ed.* **2008**, *47*, 4100–4105.
[31] P. Díaz, J. Benet-Buchholz, R. Vilar, A. J. P. White, *Inorg. Chem.* **2006**, *45*, 1617–1626.
[32] R. E. Boyett, A. P. Stevens, M. G. Ford, P. A. Cox, *Zeolites.* **1996**, *17*, 508–512.
[33] P. Jacobs, J. Martens, C. Kirschhock, *Handbook of Heterogeneous Catalysis* (Eds.: G. Ertl, H. Knözinger, F. Schüth, J. Weitkamp), Wiley-VCH, Weinheim. **2008**, pp. 160–178.
[34] Y. Kobayashi, M. Kawano, M. Fujita, *Chem. Commun.* **2006**, 4377—4379.
[35] L. Alaerts, E. Séguin, H. Poelman, F. Thibault-Starzyk, P. A. Jacobs, D. E. De Vos, *Chem. Eur. J.* **2006**, *12*, 7353–7363.
[36] S. R. Kline, *J. Appl.Crystallogr.* **2006**, *39*, 895.

Received: November 26, 2009
Published online: March 16, 2010

  